

Supporting Information

On the existence and characterization of molecular electrides

Verònica Postils, Marc Garcia-Borràs, Miquel Solà, Josep M. Luis and Eduard Matito**

* Institut de Química Computacional i Catàlisi (IQCC), Univ. Girona, Campus de Montilivi s/n, Girona, Spain. Tel: +34 972 418 357; E-mail: josepm.luis@udg.edu; ematito@gmail.com.

Contents

COMPUTATIONAL DETAILS	S1
T_{CNQLi}₂	S2
T_{CNQNa}₂	S3
Li@calix[4]pyrrole	S4
Li···NCH	S5
Li···HCN	S6
Li@B₁₀H₁₄	S7
e-@C₆₀F₆₀	S8
LINEAR AND NONLINEAR OPTICAL PROPERTIES	S9
IONIZATION POTENTIALS	S9
REFERENCES	S10

Computational Details

Geometry optimization

All geometry and single-point calculations have been performed using the Guassian09 suite of programs.¹ Geometry optimizations employed the density functional theory (DFT) Becke's three-parameter nonlocal exchange and Lee-Yang-Parr 1988 nonlocal correlation functional (B3LYP)² functional and 6-31+G(d) basis set.³ In order to ensure an accurate account of the molecular geometry, cutoffs on forces and the stepsize have been tightened;^a to improve the description of the wavefunction, the self-consistent field (SCF) convergence has also been tightened to $1 \cdot 10^{-9}$ a.u., and the grid to compute two-electron integrals and their derivatives has been augmented.^b These thresholds were applied to all systems excepting for e-@C₆₀F₆₀, whose geometry was taken from Ref. 4 and the thresholds of convergence for the SCF procedure where not tightened due to its prominent molecular size. However, the accuracy of this calculation was assessed by other means (*vide infra*).

Topological analysis and characterization of electrides

The topological quantum theory of atoms in molecules (QTAIM),⁵ electron localization function (ELF)⁶ and Laplacian of the electron density⁵ analyses were repeated at the same geometry for all the molecules but e-@C₆₀F₆₀ using aug-cc-pVDZ Dunning basis set⁷ in order to corroborate the results found. In addition, for TCNQLi₂ and TCNQNa₂ molecules additional computations at higher ab initio levels (namely, CISD and MP2 calculations in conjunction with the aug-cc-pVDZ basis set) were performed. In all cases, the qualitative results remained the same.

QTAIM and Laplacian calculations used the AIMPAC⁸ and AIMAll⁹ packages and the ToPMoD¹⁰ Package developed by Bernard Silvi and coworkers was used to compute the values of the ELF. In addition, the calculation of the electron delocalization and localization¹¹ indices was done using the results from the previous programs and the *Electron Sharing Indices Program for 3D Molecular Space Partition (ESI-3D)* developed in our group.¹²

The single-point calculation of the e-@C₆₀F₆₀ species was done using the basis of Simon et al. (used originally for the geometry optimization) that employed four s and four p functions placed in the center of the cage. In order to rule out the possibility of a basis set artifact, we performed an additional calculation using basis sets not explicitly located in the center of the structure. Namely, we placed sixty groups of three sp functions at 2.6 Å of the center of the cage, mimicking a smaller C₆₀ structure encapsulated in the cage. Both analyses of the QTAIM structure provided a NNA in the center of the cage, as well as similar pictures of ELF and the Laplacian, thus confirming the validity of the methodology employed in Ref. 4.

In the following pages we collect the full topological analyses performed in this communication.

^a We used the *verytight* option in G09 package that sets the following convergence thresholds: $1 \cdot 10^{-6}$ and $4 \cdot 10^{-6}$ a.u. for force's root mean square (RMS) and displacement's RMS values, respectively.

^b We used the *ultrafine* option in G09 package that sets a (99, 590) *pruned* grid.

TCNQLi₂

Figure S1. [top left] Topological analysis of the electron density including: the atomic positions (see labeled atoms), the bond (BCP) and ring (RCP) critical points (small spheres in grey), and the non-nuclear attractor (NNA; in red). [top right] ELF=0.75 isosurface picture indicating atomic core basins (small red spheres), valence basins (light grey) and the relevant basins for the present study (marked in green tone). [bottom] $\nabla^2\rho=-0.001$ isosurface values.

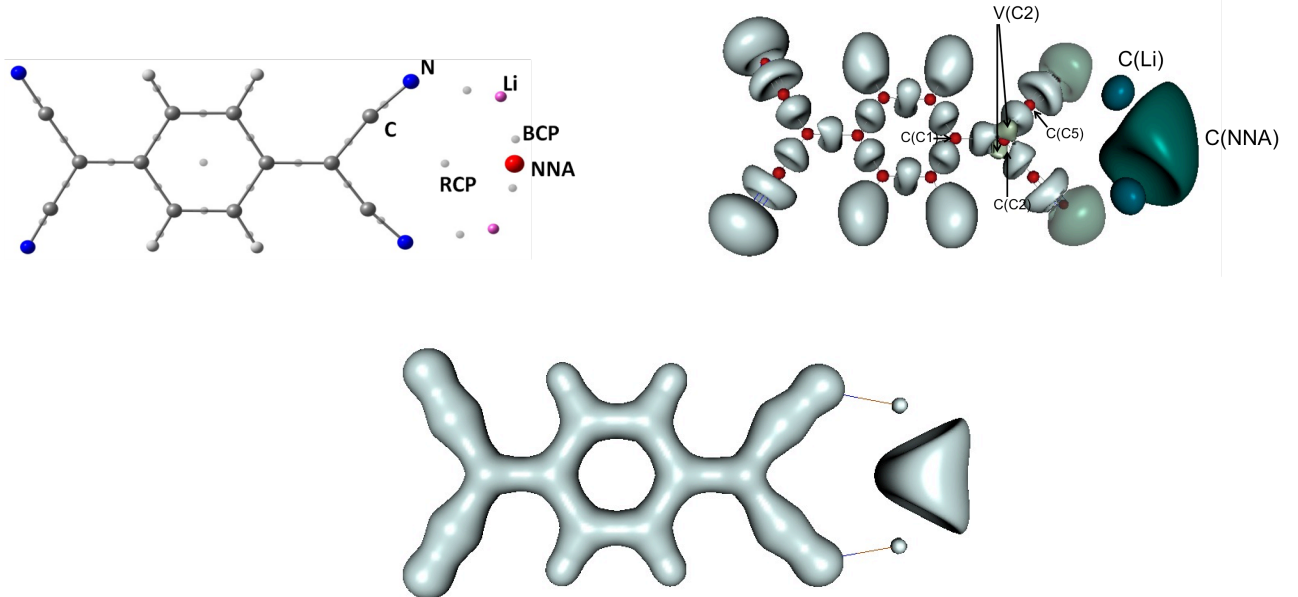


Table S1a. QTAIM and Laplacian analyses, including the distance of the lithium atoms to the NNA, ($|\vec{r}_{(NNA-Li)}|$), the values of the density ($\rho(\Omega)$) and the Laplacian of the electron density ($\nabla^2\rho$) at the Ω position, electron population of Ω ($N(\Omega)$), localization (LI) and delocalization (δ) indices and percentage of electron localization (%LI) from the total electron population. Atomic units employed.

TCNQLi ₂	Ω	$ \vec{r}_{(NNA-Li)} $	$\rho(\Omega)$	$\nabla^2\rho$	$N(\Omega)$	LI	%LI	$\delta(Li,NNA)$	$\delta(N,NNA)$
B3LYP	NNA	3.083	$9.41 \cdot 10^{-3}$	$-7.37 \cdot 10^{-3}$	0.52	0.28	51	0.20	0.05
	Li		$1.31 \cdot 10^{+1}$	$-1.70 \cdot 10^{+4}$	2.23	2.02	91		
UMP2	NNA	3.117	$9.75 \cdot 10^{-3}$	$-7.87 \cdot 10^{-3}$	0.70	0.46	67	0.16	0.06
	Li		$1.32 \cdot 10^{+1}$	$-1.70 \cdot 10^{+4}$	2.16	2.00	93		
CISD	NNA	3.147	$9.51 \cdot 10^{-3}$	$-7.60 \cdot 10^{-3}$	0.71	0.49	69		
	Li		$1.31 \cdot 10^{+1}$	$-1.70 \cdot 10^{+4}$	2.15	2.00	93		

Table S1b. Analysis of the ELF basins, Ω , including the electron population, $N(\Omega)$, the variance of the electron population, $\sigma^2(\Omega)$, the percentage of the basin's fluctuation, $\% \lambda_F(\Omega)$, and the contribution analysis of each ELF basin to the covariance with other ELF basins. Atomic units employed.

Ω	$N(\Omega)$	$\sigma^2(\Omega)$	$\% \lambda_F(\Omega)$	Contribution Analysis ($\geq 10\%$)
C(NNA)	0.92	0.20	22	C(Li) (18%), V(N,Li) (18%)
C(Li)	2.02	0.08	4	V(N,Li) (50%), C(NNA) (50%)
V(C2)	0.45	0.38	84	V(C5,C2) (24%), V(C1,C2) (21%)

TCNQNa₂

Figure S2. [top left] Topological analysis of the electron density including: the atomic positions (see labeled atoms), the bond (BCP) and ring (RCP) critical points (small spheres in grey), and the non-nuclear attractor (NNA; in red). [top right] ELF=0.75 isosurface picture indicating atomic core basins (small red spheres), valence basins (light grey) and the relevant basins for the present study (marked in green tone). [bottom] $\nabla^2\rho=-0.001$ isosurface values.

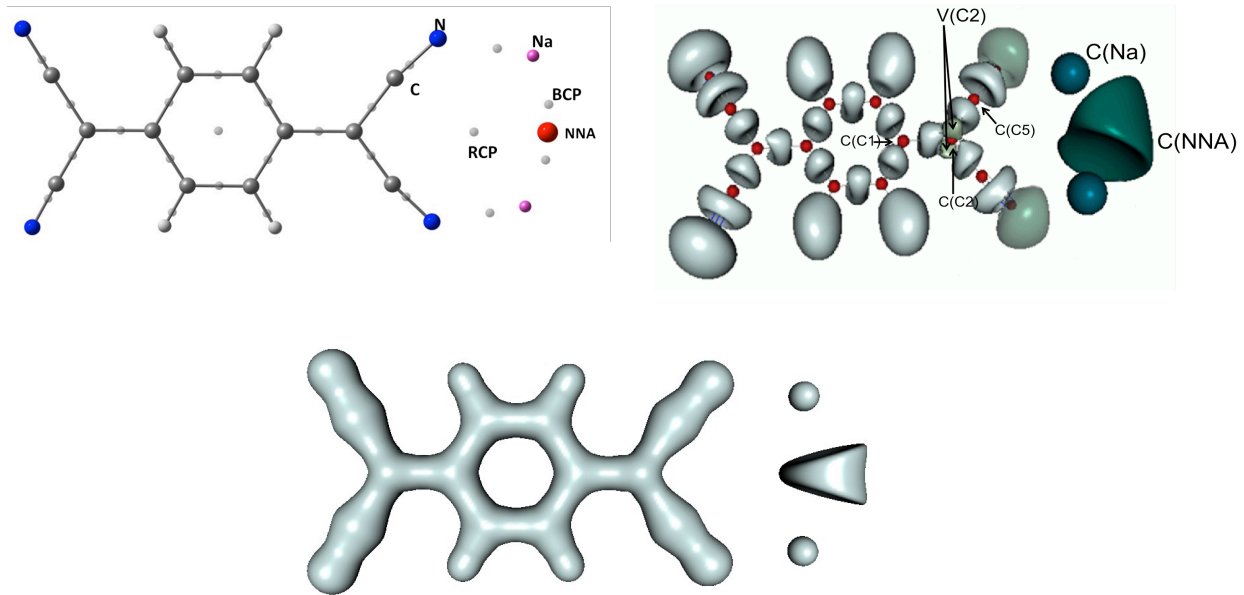


Table S2a. QTAIM and Laplacian analyses, including the distance of the sodium atoms to the NNA, ($|\vec{r}_{(NNA-Li)}|$), the values of the density ($\rho(\Omega)$) and the Laplacian of the electron density ($\nabla^2\rho$) at the Ω position, electron population of Ω ($N(\Omega)$), localization (LI) and delocalization (δ) indices and percentage of electron localization (%LI) from the total electron population. Atomic units employed.

TCNQNa ₂	Ω	$ \vec{r}_{(NNA-Li)} $	$\rho(\Omega)$	$\nabla^2\rho$	$N(\Omega)$	LI	%LI	$\delta(Li, NNA)$	$\delta(N, NNA)$
B3LYP	NNA	3.525	$6.14 \cdot 10^{-3}$	$-3.67 \cdot 10^{-3}$	0.23	0.05	22	0.16	0.02
	Na		$8.04 \cdot 10^{+2}$	$-1.78 \cdot 10^{-7}$	10.39	10.10	97		
UMP2	NNA	3.429	$6.70 \cdot 10^{-3}$	$-4.50 \cdot 10^{-3}$	0.44	0.19	43	0.22	0.02
	Na		$8.04 \cdot 10^{+2}$	$-1.78 \cdot 10^{-7}$	10.29	10.05	98		

Table S2b. Analysis of the ELF basins, Ω , including the electron population, $N(\Omega)$, the variance of the electron population, $\sigma^2(\Omega)$, the percentage of the basin's fluctuation, $\% \lambda_F(\Omega)$, and the contribution analysis of each ELF basin to the covariance with other ELF basins. Atomic units employed.

Ω	$N(\Omega)$	$\sigma^2(\Omega)$	$\% \lambda_F(\Omega)$	Contribution Analysis ($\geq 10\%$)
C(NNA)	0.89	0.26	29	C(Na) (33%)
C(Na)	10.03	0.14	1	V(N,Na) (33%), C(NNA) (67%)
V(C2)	0.44	0.38	86	V(C5,C2) (24%), V(C1,C2) (21%)

Li@calix[4]pyrrole

Figure S3. [top left] Topological analysis of the electron density including: the atomic positions (see labeled atoms), the bond (BCP) and ring (RCP) critical points (small spheres in grey), the cage critical points (small spheres in yellow) and the non-nuclear attractor (NNA; in red). [top right] ELF=0.75 isosurface picture indicating atomic core basins (small red spheres), valence basins (light grey) and the relevant basins for the present study (marked in green tone). [bottom] $\nabla^2\rho=-0.001$ isosurface values.

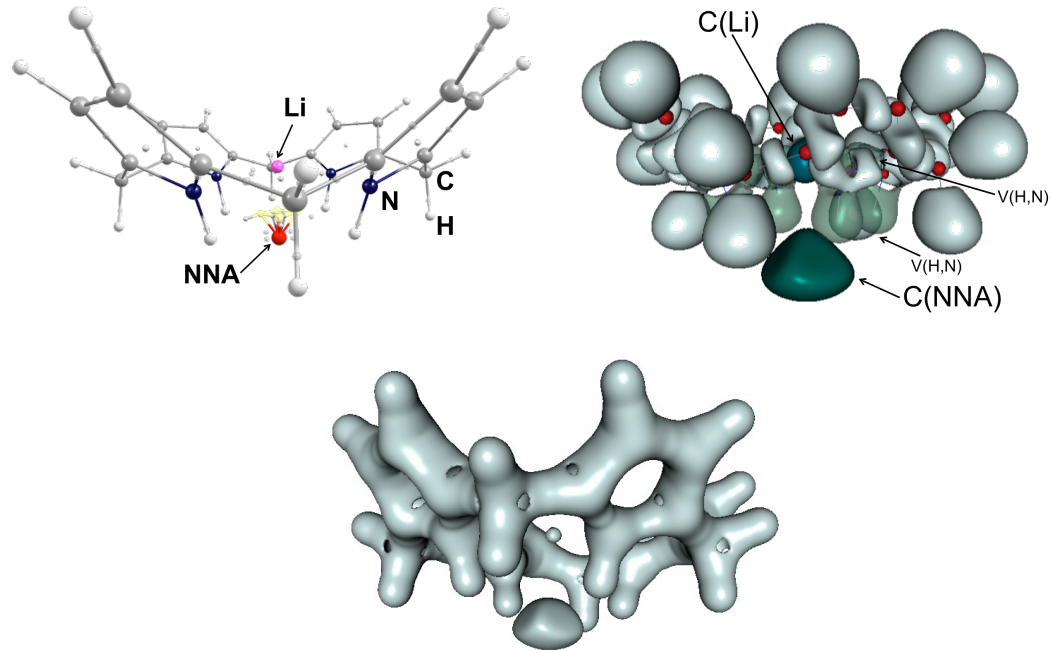


Table S3a. QTAIM and Laplacian analyses, including the distance of the lithium atom to the NNA, ($|\vec{r}_{(NNA-Li)}|$), the values of the density ($\rho(\Omega)$) and the Laplacian of the electron density ($\nabla^2\rho$) at the Ω position, electron population of Ω ($N(\Omega)$), localization (LI) and delocalization (δ) indices and percentage of electron localization (%LI) from the total electron population. Atomic units employed.

Li@calix[4]pyrrole (Ω)	$ \vec{r}_{(NNA-Li)} $	$\rho(\Omega)$	$\nabla^2\rho$	$N(\Omega)$	LI	%LI	$\delta(Li,NNA)$	$\delta(N,NNA)$
NNA	2.998	$5.61 \cdot 10^{-3}$	$-3.67 \cdot 10^{-3}$	0.15	0.02	13	0.004	0.01
Li		$1.31 \cdot 10^{+1}$	$-1.78 \cdot 10^{+7}$	2.11	1.98	94		

Table S3b. Analysis of the ELF basins, Ω , including the electron population, $N(\Omega)$, the variance of the electron population, $\sigma^2(\Omega)$, the percentage of the basin's fluctuation, $\% \lambda_F(\Omega)$, and the contribution analysis of each ELF basin to the covariance with other ELF basins. Atomic units employed.

Ω	$N(\Omega)$	$\sigma^2(\Omega)$	$\% \lambda_F(\Omega)$	Contribution Analysis ($\geq 10\%$)
C(NNA)	0.63	0.34	54	V(H,N) (17%)
C(Li)	2.03	0.08	4	V(N, Li) (20%), C(NNA) (20%)

Li···NCH

Figure S4. [top left] Topological analysis of the electron density including: the atomic positions (see labeled atoms) and the bond (BCP) critical points (small spheres in grey). [top right] ELF=0.75 isosurface picture indicating atomic core basins (small red spheres), valence basins (light grey) and the relevant basins for the present study (marked in green tone). [bottom] $\nabla^2\rho=-0.001$ isosurface values.

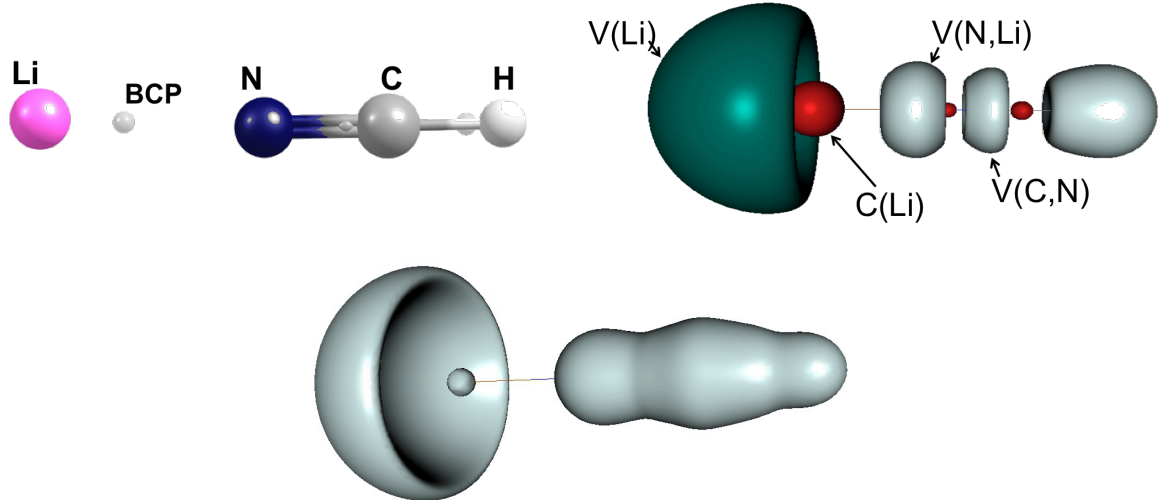


Table S4a. Analysis of the ELF basins, Ω , including the electron population, $N(\Omega)$, the variance of the electron population, $\sigma^2(\Omega)$, the percentage of the basin's fluctuation, $\% \lambda_F(\Omega)$, and the contribution analysis of each ELF basin to the covariance with other ELF basins. Atomic units employed.

Ω	$N(\Omega)$	$\sigma^2(\Omega)$	$\% \lambda_F(\Omega)$	Contribution Analysis ($\geq 10\%$)
V(Li)	0.91	0.16	18	V(N,Li) (46%), C(Li) (38%), V(C,N) (15%)
C(Li)	2.02	0.08	4	V(N, Li) (37%), V(Li) (62%)

Li...HCN

Figure S5. [top left] Topological analysis of the electron density including: the atomic positions (see labeled atoms) and the bond (BCP) critical points (small spheres in grey). [top right] ELF=0.75 isosurface picture indicating atomic core basins (small red spheres), valence basins (light grey) and the relevant basins for the present study (marked in green tone). [bottom] $\nabla^2\rho=-0.002$ isosurface values.

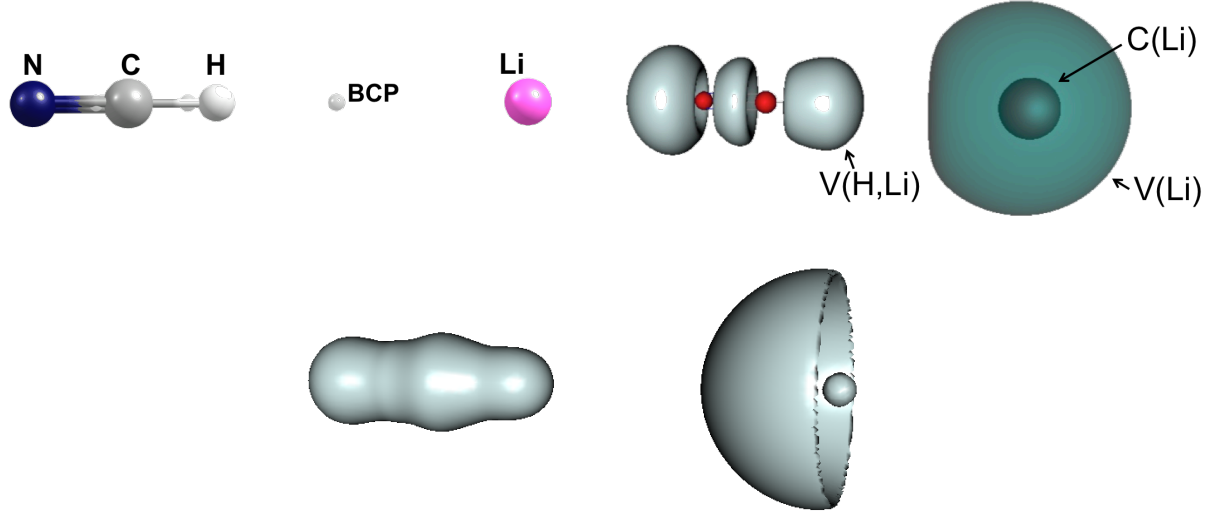


Table S5a. Analysis of the ELF basins, Ω , including the electron population, $N(\Omega)$, the variance of the electron population, $\sigma^2(\Omega)$, the percentage of the basin's fluctuation, $\% \lambda_F(\Omega)$, and the contribution analysis of each ELF basin to the covariance with other ELF basins. Atomic units employed.

Ω	$N(\Omega)$	$\sigma^2(\Omega)$	$\% \lambda_F(\Omega)$	Contribution Analysis ($\geq 10\%$)
V(Li)	0.95	0.11	12	C(Li) (75%), V(H,C) (25%)
C(Li)	2.01	0.06	3	V(Li) (98%)

Li@B₁₀H₁₄

Figure S6.[top left] Topological analysis of the electron density including: the atomic positions (see labeled atoms), the bond (BCP) and ring (RCP) critical points (small spheres in grey) and the cage critical points (small spheres in yellow). [top right] $\nabla^2\rho=-0.001$ isosurface values. [bottom] ELF=0.75 isosurface picture (**left**) and ELF=0.20 isosurface picture (**center**) indicating atomic core basins (small red spheres), valence basins (light grey) and the relevant basins for the present study (marked in green tone). (**right**) 2D contour plot of the ELF function.

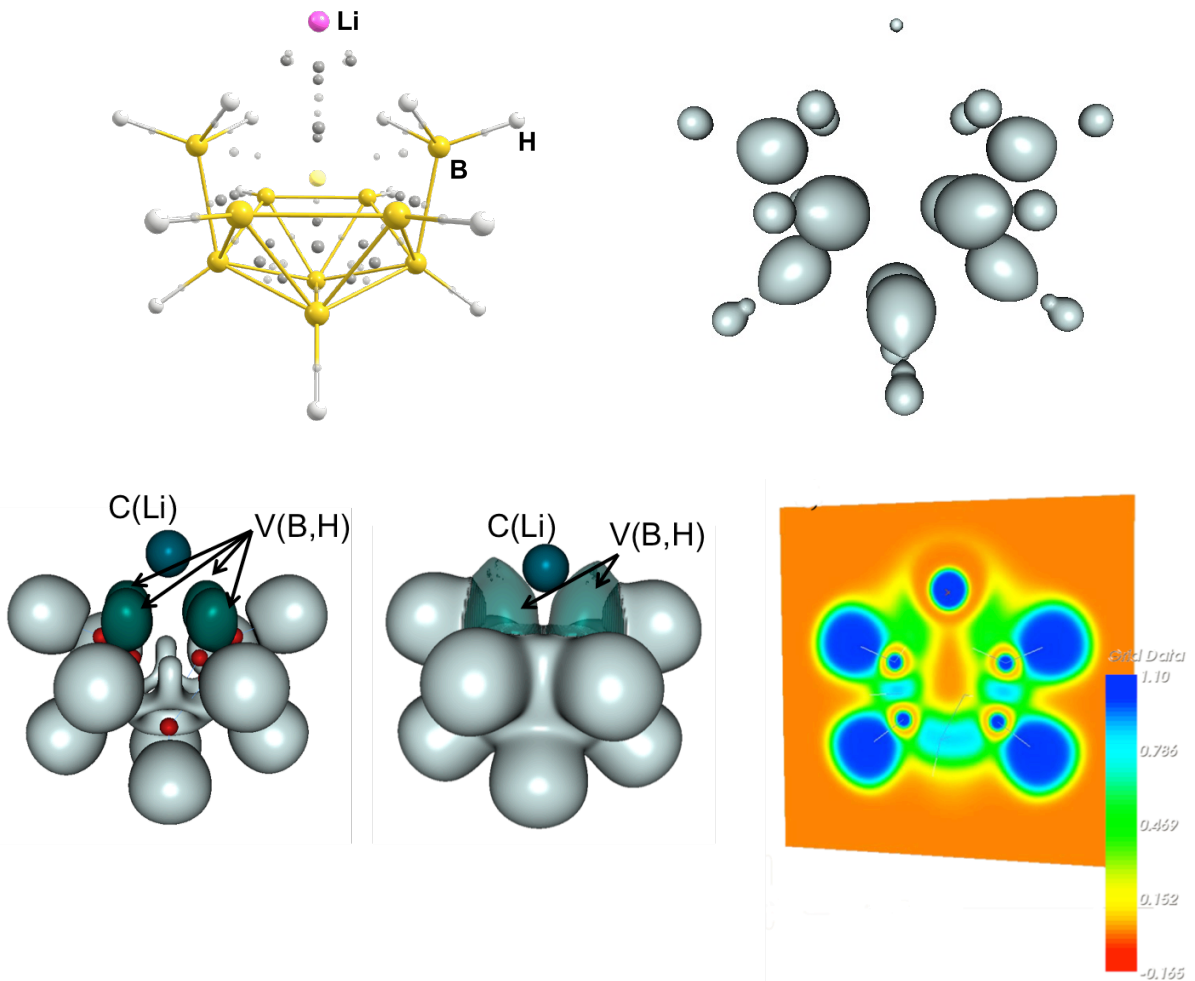


Table S6a. Analysis of the ELF basins, Ω , including the electron population, $N(\Omega)$, the variance of the electron population, $\sigma^2(\Omega)$, the percentage of the basin's fluctuation, $\% \lambda_F(\Omega)$, and the contribution analysis of each ELF basin to the covariance with other ELF basins. Atomic units employed.

Ω	$N(\Omega)$	$\sigma^2(\Omega)$	$\% \lambda_F(\Omega)$	Contribution Analysis ($\geq 10\%$)
C(Li)	2.02	0.06	3	V(B,H) (25%) each
V(B,H)	2.04	0.84	41	V(B,H) (14%), others not relevant

e-@B₁₀H₁₄

Figures S7. [top left] Topological analysis of the electron density including: the atomic positions (see labeled atoms), the bond (BCP) and ring (RCP) critical points (small spheres in grey), the cage critical points (small spheres in yellow) and the non-nuclear attractor (NNA; in red). [top right] ELF=0.75 isosurface picture indicating valence basins (light grey) and the isolated-electron of the electride basin (marked in green). [bottom] $\nabla^2\rho=-0.001$ isosurface values.

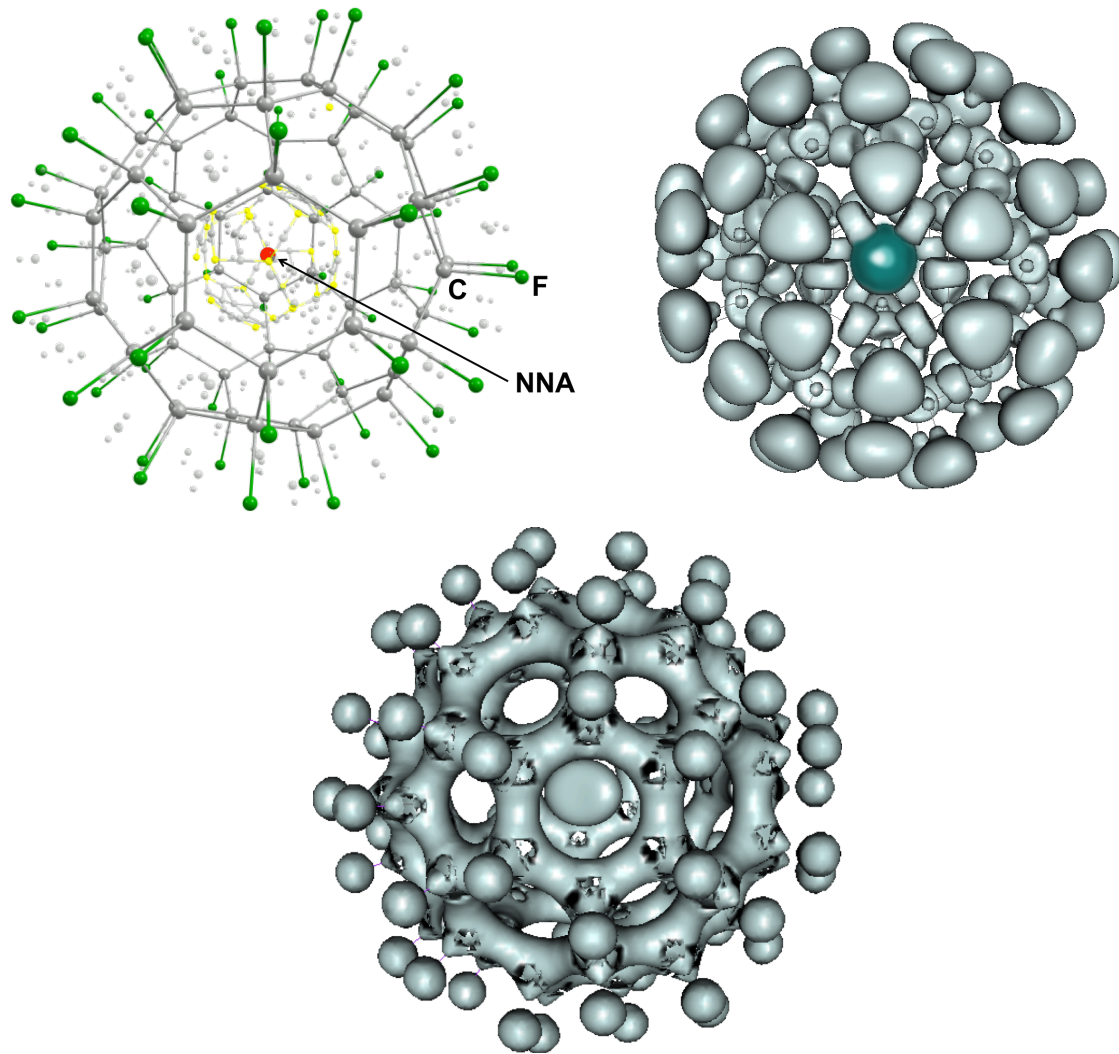


Table S7a. QTAIM and Laplacian analyses for the e-@C₆₀F₆₀ including: the values of the density ($\rho(\Omega)$) and the Laplacian of the electron density ($\nabla^2\rho$) at the Ω position, electron population of Ω ($N(\Omega)$), the localization (LI) index and the percentage of electron localization (%LI) from the total electron population. Atomic units employed.

e-@C ₆₀ F ₆₀ (Ω)	$\rho(\Omega)$	$\nabla^2\rho$	$N(\Omega)$	LI	%LI
NNA	$1.74 \cdot 10^{-3}$	$-2.63 \cdot 10^{-4}$	0.19	0.03	18

Linear and Nonlinear Optical Properties

Table S8. Electronic contribution to linear and nonlinear optical properties (NLOP) for the molecules studied in this communication. ^aData from Ref. 13. ^bData from Ref. 4. ^cData from Ref. 14. ^dValues computed at the UB3LYP/aug-cc-pVDZ level of theory.

properties	TCNQLi ₂ ^a	TCNQNa ₂ ^a	Li@Calix ^a	Li@B ₁₀ H ₁₄ ^a	Li···HCN ^c	HCN···Li ^c	Li ₂ (S=0)	Li ₂ (S=0)
α_{zz} (0;0)					212.6	158.2	263.2	583.0
$\vec{\alpha}$ (0; 0)	371.9	389.7	381.6	150.3	181.9	239.1	198.5	340.0
β_{zzz} (0;0,0)					-2791	-3640		
γ_{zzzz} (0;0,0,0)							1.2·10 ⁶	9.2·10 ⁵
γ_{\parallel} (0; 0,0)	1.4·10 ⁶	1.3·10 ⁶	4.8·10 ⁶	4.8·10 ⁵				

Ionization Potentials

Table S9. Ionization Potentials for the molecules studied in this work computed at the B3LYP/aug-cc-pVDZ level of theory. ^aComputed at the level of theory of Ref. 4.

molecule	PI (eV)
TCNQLi ₂	(S=1 → S=1/2) 6.32
	(S=1 → S=3/2) 7.80
TCNQNa ₂	(S=1 → S=1/2) 6.11
	(S=1 → S=3/2) 7.47
Li@Calix	(S=1/2 → S=0) 3.82
Li@B ₁₀ H ₁₄	(S=1/2 → S=0) 6.39
e-@C ₆₀ F ₆₀ ^a	(S=1/2 → S=0) 3.99
Li···HCN	(S=1/2 → S=0) 5.98
HCN···Li	(S=1/2 → S=0) 4.35

References

- [1.] M. J. FRISCH, G. W. TRUCKS, H. B. SCHLEGEL, G. E. SCUSERIA, M. A. ROBB, J. R. CHEESEMAN, G. SCALMANI, V. BARONE, B. MENNUCCI, G. A. PETERSSON, H. NAKATSUJI, M. CARICATO, X. LI, H. P. HRATCHIAN, A. F. IZMAYLOV, J. BLOINO, G. ZHENG, J. L. SONNENBERG, M. HADA, M. EHARA, K. TOYOTA, R. FUKUDA, J. HASEGAWA, M. ISHIDA, T. NAKAJIMA, Y. HONDA, O. KI-TAO, H. NAKAI, T. VREVEN, J. A. MONTGOMERY, JR., J. E. PERALTA, F. OGLIARO, M. BEARPARK, J. J. HEYD, E. BROTHERS, K. N. KUDIN, V. N. STAROVEROV, R. KOBAYASHI, J. NORMAND, K. RAGHAVACHARI, A. RENDELL, J. C. BURANT, S. S. IYENGAR, J. TOMASI, M. COSSI, N. REGA, J. M. MILLAM, M. KLENE, J. E. KNOX, J. B. CROSS, V. BAKKEN, C. ADAMO, J. JARAMILLO, R. GOMPERTS, R. E. STRATMANN, O. YAZYEV, A. J. AUSTIN, R. CAMMI, C. POMELLI, J. W. OCHTERSKI, R. L. MARTIN, K. MOROKUMA, V. G. ZAKRZEWSKI, G. A. VOTH, P. SALVADOR, J. J. DANNENBERG, S. DAPPRICH, A. D. DANIELS, Å. FARKAS, J. B. FORESMAN, J. V. ORTIZ, J. CIOSLOWSKI, and D. J. FOX, Gaussian 09 Revision A.1, Gaussian Inc. Wallingford CT 2009.
- [2.] A. D. BECKE, *J. Chem. Phys.* **98**, 5648 (1993).
- [3.] R. DITCHFIELD, W. J. HEHRE, and J. A. POPLE, *J. Chem. Phys.* **54**, 724 (1971). ; W. J. HEHRE, R. DITCHFIELD, and J. A. POPLE, *J. Chem. Phys.* **56**, 2257 (1972). ; P. C. HARIHARAN and J. A. POPLE, *Theor. Chim. Acta (Berlin)* **28**, 213 (1973). ; M. M. FRANCL, W. J. PIETRO, W. J. HEHRE, J. S. BINKLEY, M. S. GORDON, D. J. DEFREES, and J. A. POPLE, *J. Chem. Phys.* **77**, 3654 (1982).
- [4.] Y.-F. WANG, Z.-R. LI, D. WU, C.-C. SUN, and F.-L. GU, *J. Comput. Chem.* **31**, 195 (2010).
- [5.] R. F. W. BADER and T. T. NGUYEN-DANG, Quantum Theory of Atoms in Molecules –Dalton Revisited, in *Advances in Quantum Chemistry*, volume 14, pp. 63–124, Academic Press, New York, 1981.
- [6.] A. D. BECKE and K. E. EDGEcombe, *J. Chem. Phys.* **92**, 5397 (1990).
- [7.] R. A. KENDALL, T. H. DUNNING JR, and R. J. HARRISON, *J. Chem. Phys.* **96**, 6796 (1992).
- [8.] F. W. BIEGLER-KONIG, T. T. NGUYEN-DANG, Y. TAL, and R. F. W. BADER, *J. Phys. B: Atom. Molec. Phys.* **14**, 2739 (1981). ; F. W. BIEGLER-KÖNIG, R. F. BADER, and T.-H. TANG, *J. Comput. Chem.* **3**, 317 (1982).
- [9.] T. A. KEITH, AIMall (Version 14.11.23), 2014, TK Gristmill Software, Overland Park KS, USA (aim.tkgristmill.com).
- [10.] S. NOURY, X. KROKIDIS, F. FUSTER, and B. SILVI, TopMoD package, 1997.
- [11.] E. MATITO and M. SOLÀ, *Coord. Chem. Rev.* **253**, 647 (2009); E. MATITO, M. DURAN, and M. SOLÀ, *J. Chem. Phys.* **122**, 014109 (2005); E. MATITO, M. SOLÀ, P. SALVADOR, and M. DURAN, *Faraday Discuss.* **135**, 325 (2007); F. FEIXAS, E. MATITO, M. DURAN, M. SOLÀ, and B. SILVI, *J. Chem. Theory Comput.* **6**, 2736 (2010).
- [12.] E. MATITO, ESI-3D: Electron Sharing Indices Program for 3D Molecular Space Partitioning; Institute of Computational chemistry and Catalysis, University of Girona, Catalonia, Spain, 2006.
- [13.] M. GARCIA-BORRÀS, M. SOLÀ, J. M. LUIS, and B. KIRTMAN, *J. Chem. Theory Comput.* **8**, 2688 (2012).
- [14.] W. CHEN, Z.-R. LI, D. WU, R.-Y. LI, and C.-C. SUN, *J. Phys. Chem. B* **109**, 601 (2005).